

Anisotropic conductivity on diblock copolymers with lamellar microdomains

Koji Ishizu*, Yoshikuni Yamada and Reiko Saito

Department of Polymer Science, Tokyo Institute of Technology, 2-12, Ookayama, Meguro-ku, Tokyo 152, Japan

and Takaki Kanbara and Takakazu Yamamoto

Research Laboratory of Resource Utilization, Tokyo Institute of Technology, 4259 Nagatsuda, Midori-ku, Yokohama 227, Japan

(Received 10 February 1992; revised 6 October 1992)

Well-defined poly(styrene-*b*-2-vinylpyridine) diblock copolymers (about 50 wt% polystyrene blocks) were prepared by sequential anionic addition. The cast films showed a tendency where the alternating lamellar structures of two microphases were orientated with their interfaces parallel to the surface that contacts the air or Teflon substrate. Poly(2-vinylpyridine) microdomains were not only quaternized but also effectively crosslinked with 1,4-diodobutane vapour. Subsequently, colloidal silver was introduced into quaternized poly(2-vinylpyridine) phases by the reduction of silver iodide. The element distributions on the vertical section of the modified films were measured by means of energy-dispersive X-ray spectrometer and transmission electron microscopy. These materials showed a highly anisotropic conductivity with ca. six orders of magnitude.

(Keywords: diblock copolymer; lamellar structure; colloidal silver; energy dispersive X-ray spectrometer; transmission electron microscopy; anisotropic conductivity)

INTRODUCTION

Many of the available conductive polymers possess some undesirable characteristics, such as environmental instability, poor processability or poor physical properties¹⁻⁴. There have been reports of attempts to improve the physical properties of these conductive polymers by using block copolymers in which one of the blocks consists of a conducting sequence^{5,6}. Generally, such block copolymers form a microphase-separated structure in the solid state owing to incompatible block chains. Möller and Lenz⁷, and Stankovic *et al.*⁸ have reported the electrical conductivity of diblock copolymers (macroscopically orientated lamellae) in which one of the blocks consisted of poly(2-vinylpyridine) (P2VP). In addition, semiconducting materials were obtained upon exposure of block copolymer films to iodine vapour. However, these materials have never shown electrical anisotropy with conductivities. Shimidzu *et al.*⁹ have reported that the amphiphilic pyrrole LB film (200 layers) showed a highly anisotropic conductivity with ca. ten orders of magnitude (conductivity parallel to multilayer: $\sigma_{\parallel} = 10^{-1} \text{ S cm}^{-1}$; conductivity in the perpendicular direction: $\sigma_{\perp} = 10^{-11} \text{ S cm}^{-1}$).

More recently, we have made clear that poly[styrene(S)-*b*-isoprene(I)] and poly[S-*b*-2-vinylpyridine(2VP)] diblock copolymers (about 50 wt% polystyrene (PS) blocks and relatively narrow molecular weight distribution) formed horizontally orientated lamellar microdomains by means of the air-copolymer and the substrate-

copolymer interactions¹⁰. Subsequently, semiconducting materials were obtained upon exposure of a block copolymer film with the vapour of alkyl halides. The quaternized P2VP domains of these films exhibited the nature of ionic conduction¹¹. This film had an anisotropic conductivity with ca. eight orders of magnitude ($\sigma_{\parallel} = 1.7 \times 10^{-6}$ and $\sigma_{\perp} = 5.6 \times 10^{-14} \text{ S cm}^{-1}$).

For this article, we fabricated the cast film exhibiting horizontally orientated lamellar microdomains of poly(S-*b*-2VP) diblock copolymers. P2VP microdomains were not only quaternized but also crosslinked with 1,4-diodobutane (DIB) vapour. Colloidal silver was introduced into quaternized P2VP phases by reduction of silver iodide. Morphological results were obtained by a transmission electron microscope (TEM) on a vertical section of modified film. The element distributions on a vertical section of the films were measured by energy dispersive X-ray spectrometry (e.d.x.). The anisotropic conductivity on these materials was studied in detail.

EXPERIMENTAL

Polymer synthesis and characterization

The well-defined poly(S-*b*-2VP) diblock copolymers were prepared by the usual sequential anionic addition polymerization using *n*-butyllithium as an initiator in tetrahydrofuran (THF) at -78°C . The details concerning the synthesis and characterization of such block copolymers have been given elsewhere¹⁰⁻¹². Table 1 lists the characteristics of 'monodisperse' diblock copolymers exhibiting lamellar microdomains and the microdomain

* To whom correspondence should be addressed

Table 1 Characteristics and domain size of poly(S-*b*-2VP) diblock copolymers

Specimen code	$10^{-5} \overline{M}_n^a$	Content of PS block (wt%)	$\overline{M}_w/\overline{M}_n^a$	Casting solvent	Shape	Domain size (nm) ^b	
						\overline{D}_{PS}	\overline{D}_{P2VP}
SV1	1.0	47.0	1.13	CHCl ₃ /dioxane 6/4 (v/v)	lamellae	25	27
SV2	2.0	32.8	1.13	TCE	lamellae	53	37

^a Determined by g.p.c. using universal calibration

^b \overline{D}_{PS} (\overline{D}_{P2VP}), average domain distance of PS (P2VP) lamellae

size of a specimen cast from chloroform(CHCl₃)/dioxane mixture or 1,1,2-trichloroethane (TCE).

Morphology of diblock copolymer films

The morphology of block copolymers strongly depends on the thermal history in the preparation process. In a previous work¹⁰, we found that CHCl₃/dioxane 6/4 (v/v) mixture works as a non-selective solvent for both PS and P2VP components. So SV1 film (PS 47.0 wt%, 40 μm thick) was cast from a 0.03 g ml⁻¹ CHCl₃/dioxane mixture with a Teflon sheet (0.11 ml cm⁻²) as a substrate. The casting solvent was evaporated as gradually as possible under saturated vapour. On the other hand, SV2 film (PS 32.8 wt%) was cast from TCE solution, and the TCE seems to work somewhat poorly for the P2VP component. Annealing treatment was not carried out for these films. Next, the films were embedded in an epoxy resin and cut perpendicularly to the film interfaces into ultra-thin sections (about 70–100 nm thick) using an ultramicrotome (Reichert-Nissei Co, Ultracut N). Morphological results were obtained with a Hitachi H-500 TEM at 75 kV.

Introduction of colloidal silver to P2VP phases

Diblock copolymer films (90–160 μm thick) cast on Teflon sheet were dried for three days under a high vacuum. Quaternization of P2VP domains was carried out by alkyl halide compounds. At first, the film was exposed to DIB vapour at 60°C under a reduced pressure. This reagent led not only to quaternization but also to crosslinking of P2VP microdomains. Subsequently, the unreacted P2VP parts of the lamellar domains were quaternized with methyl iodide vapour at room temperature for three days. The degree of quaternization was determined by Volhard's titration as follows. The crosslinked film was swollen in benzene for two days. In order to cause the swollen film to scission, this solution was exposed to ultrasonic irradiation (USH 3002-20S, 300 W, 19 Hz, Choonpa Kogyo Co. Ltd) for 15 min.

Crosslinked films (ca. 20 mg) were soaked in dioxane/water 1/10 (v/v) mixture solution of silver acetate (AgAc) for 8–18 h in the dark. Subsequently, the film was washed with water and dried at 30°C in the dark. This film was soaked in a dioxane/water 1/10 (v/v) mixture of hydroquinone (2.5 wt%) for 2 h at 20°C. The film was washed with water and soaked in aqueous sodium bisulfite (Na₂S₂O₃, 5 wt%) for 1–5 h at 20°C. This film was washed with water for 10 min and dried *in vacuo*.

Next, the film was broken in liquid nitrogen. The element (silver, iodine and sulfur) distributions on the vertical section of the films were measured by e.d.x. (Philips EDAX 9900I). We used a highly flat surface on the specimen within the possible limits of the

measurements. The flatness of the specimen surface is essential for quantitative analysis, since surface irregularity affects the matrix corrections, especially those for X-ray absorption and electron backscattering. The K intensity was fitted with a Zn atom ($K_\alpha = 8.628$ and $L_\alpha = 1.019$ keV). The mass concentration of the elements was estimated using ZAF correction (stopping power, absorption, and fluorescence corrections: RT-11 SJ(S) V05.01C) on a computer (LSI-11/23 computer).

Conductivity of modified films

The sample film would behave as a two-dimensional conductor (conductivity parallel to the film plane σ_{\parallel} and conductivity perpendicular to film plane σ_{\perp}) due to the structure of horizontally orientated lamellae. The measurement method and instruments for conductivities were given in a previous report¹¹.

RESULTS AND DISCUSSION

Figures 1a and 1c show cross-sections of the SV1 film cast from CHCl₃/dioxane 6/4 (v/v) mixture near the air-copolymer interface (micrograph a) and near the Teflon substrate-copolymer interface (micrograph c), respectively. The upper and lower arrows indicate the free surface of the film and the surface that contacts the Teflon substrate, respectively. Figure 1b is an enlargement of the frame portion in micrograph 1c. The dark portions are the selectively stained P2VP blocks with osmium tetroxide (OsO₄). The thermal equilibrium morphology of SV1 film (PS blocks 47.0 wt%) is an alternating lamellar structure of P2VP and PS microphases. The distribution of P2VP and PS domain sizes is very uniform due to the monodispersity ($\overline{M}_w/\overline{M}_n = 1.13$) of the SV1 diblock copolymer. It is found from these micrographs that the alternating lamellae of PS and P2VP microphases are orientated with their interfaces parallel not only in the surfaces that contact the air and substrate but also in bulk. It was also recognized from X-ray photoelectron spectroscopy studies^{10,11}, that the outermost layer consisted of a single layer of PS block chains having lower solid-state surface tension. The PS layer was aligned with its interface parallel to the surface that contacted the Teflon substrate.

Figure 2 shows a cross-section (in bulk) of the SV2 film (PS blocks 32.8 wt%) cast from TCE on the Teflon substrate. Even in this specimen, the diblock copolymer forms the same horizontally orientated lamellar microdomains as the SV1 specimen. The PS layer was aligned with its interface parallel not only to the free surface but also to the substrate surface. The TCE works somewhat poorly for the P2VP component.

P2VP microdomains of the SV1 film were not

Table 2 Reaction conditions and results of introduction of colloidal silver into quaternized SV films

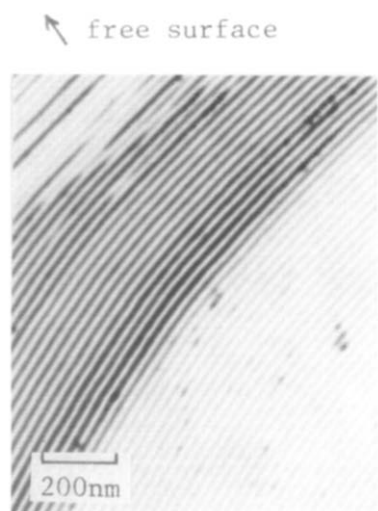
Run no.	Film			AgAc		Soaking time (h)	Soaking time in hydroquinone (h)	Soaking time in Na ₂ S ₂ O ₃ (h)	Introduced ^d ratio of [Ag]/[QPy] (mol/mol)
	DQ ^a (mol%)	Crosslinking ^b density (%)	Weight (mg)	[AgAc] 10 ² (mol l ⁻¹)	[AgAc]/[QPy] ^c (mol/mol)				
SV1-E1	69.0	47.3	25.0	0.6	3	8	2	5	0.06
SV2-E1	47.1	35.2	23.5	6.0	20	18	2	5	–
SV2-E2	47.1	35.2	19.0	6.0	20	18	2	0	1.02
SV2-E3	47.1	35.2	26.0	6.0	20	18	2	1	0.82

^a DQ, degree of quaternization, was determined by Volhard's titration

^b Calculated from the difference between DQ and pendant I-groups determined by Volhard's titration in benzene and triethylamine mixture

^c Mole ratio of AgAc to pyridinium units

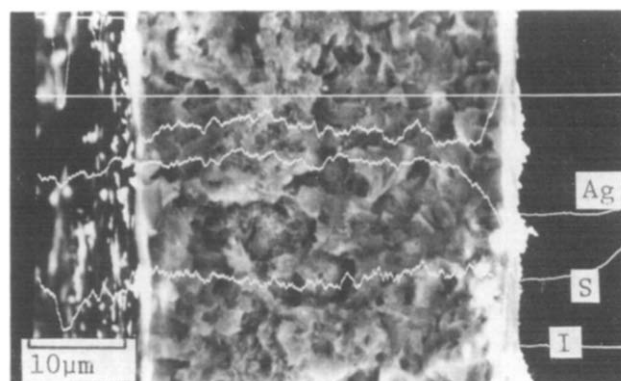
^d Determined by Volhard's titration after scission of the swollen films

**Figure 4** Cross-sectional TEM micrograph of SV1-E1 film

Silver iodide (AgI) is introduced to the quaternized P2VP phases by the ion-exchange reaction of pyridinium ion with AgAc (equation (1)). The AgI salts produced are reduced to Ag metal and I⁻ ion with hydroquinone (equation (2)). In this reduction stage, the residual AgAc is also reduced to Ag metal and I⁻ ion (equation (3)). At the final fixing stage, the unreacted Ag⁺ ion is converted to the Ag(S₂O₃)₂³⁻ ion given by equation (4) and removed to be free from the film.

The crosslinking densities of SV1-E and SV2-E films were 47.3 and 35.2 mol%, respectively. A dioxane/water mixture was used as the solvent. Both SV1-E and SV2-E films were broken down in dioxane/water 2/10 (v/v) mixture due to high swelling of PS layers. Consequently, we adopted in this work the following solvent composition: dioxane/water 1/10 (v/v). In this composition, the apparent degree of swelling for both films was almost the same as that for dry films, but the PS layers would be able to swell microscopically.

The concentration of AgAc ([AgAc]) and the mole ratio of AgAc to pyridinium units ([AgAc]/[QPy]) were varied from 0.6×10^{-2} – 6.0×10^{-2} mol l⁻¹ and 3–20 mol/mol, respectively. After soaking in AgAc solution, the films turned ash-coloured and the weights of every film increased. It was suggested that AgI was formed in the film. The film turned metallic black after the reduction with hydroquinone. Finally, the removal

**Figure 5** E.d.x. data (b.s.e. image of Ag atoms and concentration distributions of Ag, I and S atoms) of SV1-E1 fragment

of unreacted AgI from the film was carried out with aqueous Na₂S₂O₃.

Figure 4 shows a cross-section of the SV1-E1 film ([AgAc] = 0.6×10^{-2} mol l⁻¹, [AgAc]/[QPy] = 3 mol/mol) after the treatment of Na₂S₂O₃. The dark, grey and white portions indicate silver, quaternized P2VP, and PS blocks, respectively. It was found from this micrograph that a lot of colloidal silver is introduced into the quaternized P2VP layers near the film surface. The colloidal silver has never been observed in the quaternized P2VP layers near the bulk. Moreover, the colloidal silver has also never been observed in PS layers. Typical e.d.x. data of SV1-E1 fragments are shown in *Figure 5*. It is also seen that the concentration of Ag on the white scanning line is localized with a large amount in both sides near the film surface. The concentration distributions of I and S atoms are almost constant on the white scanning line. The introduced ratio of [Ag]/[QPy] is 0.06 mol/mol as listed in *Table 2*. The introduced amount of colloidal silver is very small in this reaction condition.

The SV2-E1 film was soaked in a high concentration of AgAc ([AgAc] = 6.0×10^{-2} mol l⁻¹, [AgAc]/[QPy] = 20 mol/mol) for a long time (18 h). *Figure 6* shows a cross-section of the SV2-E1 film after the treatment of Na₂S₂O₃. In contrast with the SV1-E1 specimen, a lot of colloidal silver is introduced into the quaternized P2VP layers in bulk. *Figure 7* shows the e.d.x. data ((a) b.s.e. image of Ag atoms; (b) spot analysis of the centre; (c) spot analysis of the right-edge). It was found from the b.s.e. image (micrograph (a)) that a large amount of

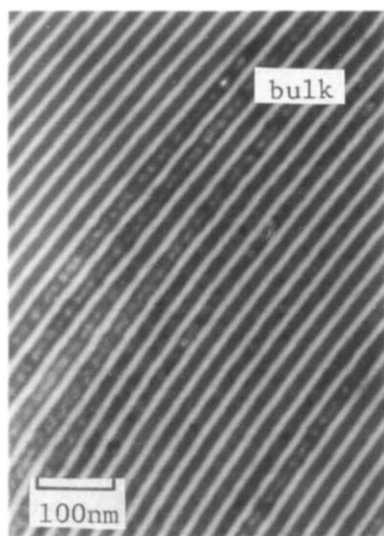


Figure 6 Cross-sectional TEM micrograph of SV2-E1 film

colloidal silver is localized near the centre of the film. The e.d.x. data agree well with TEM results for the concentration gradient of the Ag atom. These phenomena are also supported by the results of the spot analyses shown in Figures 7b and 7c. On the other hand, the I content is almost constant regardless of the position of the film, but its amount is very small. It is found therefore that I^- ions are excluded from the film. The S content at the right-edge is larger than that at the centre. This result indicates that $Na_2S_2O_3$ used at fixing stage (equation (4)) still exists near the surface of the film.

Consequently, it seems to be better for the introduction conditions of colloidal silver that both values of $[AgAc]$ and $[AgAc]/[QPy]$ are high, and the fixing time with aqueous $Na_2S_2O_3$ is short. The e.d.x. of SV2-E film was measured stepwise at the development and fixing stages. Figure 8 shows the e.d.x. data of SV2-E2 fragments (after development). The micrograph indicates the concentration distributions of Ag and I atoms superimposed in the b.s.e. image of Ag atoms. It was found from the concentration distribution of Ag that Ag atoms are localized with the rich amount near both edges of the film. From the b.s.e. image, Ag atoms are introduced homogeneously into the bulk. However, their absolute amounts are small compared with those of both sides near the film surfaces. The introduced ratio of $[Ag]/[QPy]$ was obtained to be 1.02 mol/mol from Volhard's titration (see Table 2). This result indicates that not only the produced AgI, but also residual AgAc, were reduced with hydroquinone according to equation (2) and equation (3), respectively. Figure 9 shows the spot analyses of Ag and I atoms ((a) right-edge; (b) left-edge; (c) centre). It was found from these spectra that the observed value of I/Ag at the centre decreased in comparison with those at both edges. This means that the reduced I^- ions are excluded free with a large amount from the film at the reduction stage (equation (2)). It is made clear from these results that both the AgI and residual AgAc produced are distributed in rich amounts at both sides near the film surfaces during the ion-exchange reaction (equation (1)) because the diffusion rates of AgAc and $Na_2S_2O_3$ are extremely slow in the bulk of the film.

Next, we measured the e.d.x. of SV2-E3 fragments. The

SV2-E3 film corresponds to the film after $Na_2S_2O_3$ treatment (fixing stage) of SV2-E2. Figure 10 shows the e.d.x. data of SV2-E3 fragments. The micrograph indicates the concentration distributions of Ag, I and S atoms superimposed in the b.s.e. image of Ag atoms. It was found from this micrograph that Ag atoms are localized with rich amounts in both sides near the film surfaces. It was also found from the b.s.e. image that Ag atoms are introduced homogeneously in quaternized P2VP layers near the bulk after fixing treatment (soaking time, 1 h), although the absolute amount is small. The introduced ratio of $[Ag]/[QPy]$ was found to be

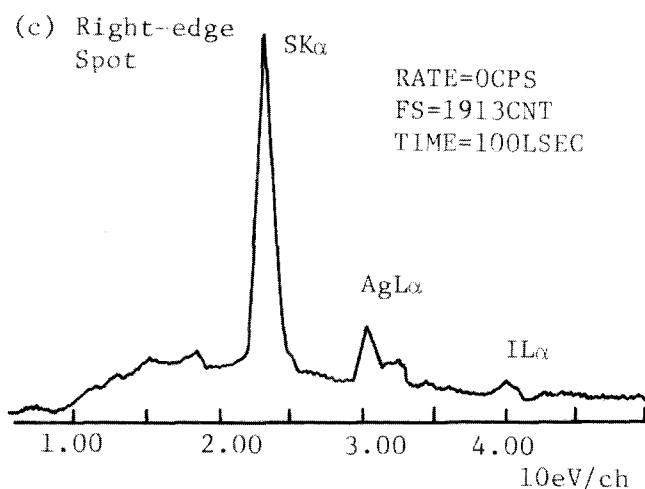
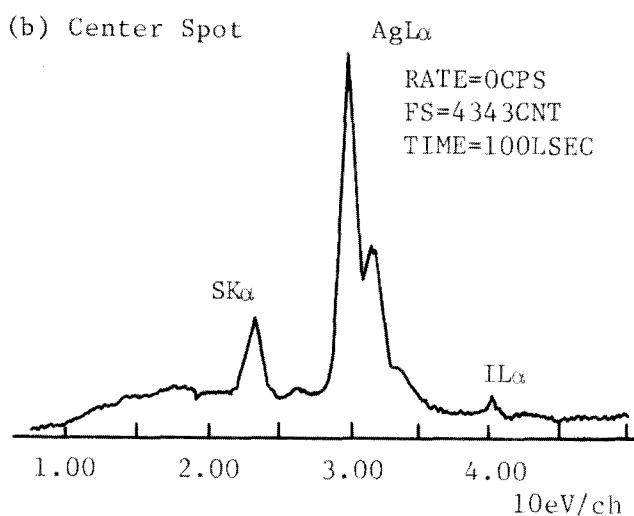
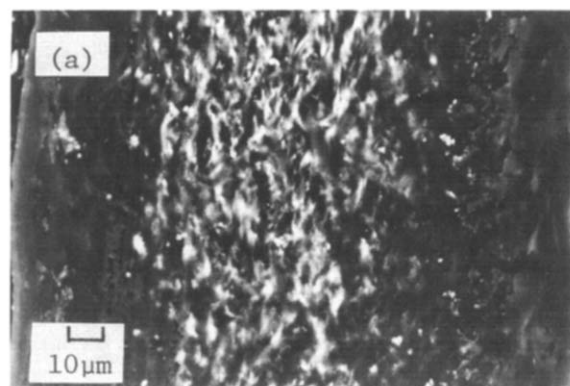


Figure 7 E.d.x. data of SV2-E1 fragment: (a) b.s.e. image of Ag atoms; (b) spot analysis of the centre; (c) spot analysis of the right-edge

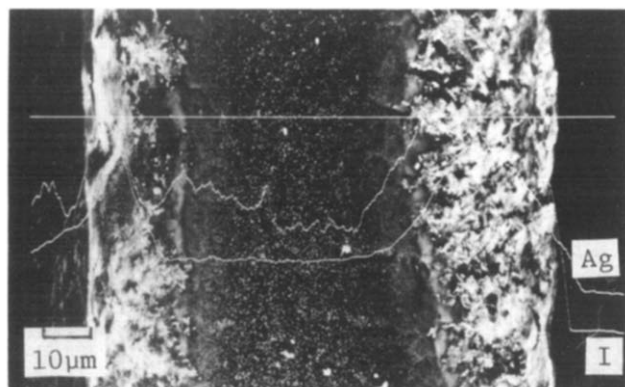


Figure 8 E.d.x. data (b.s.e. image of Ag atoms and concentration distributions of Ag and I atoms) of SV2-E2 fragment

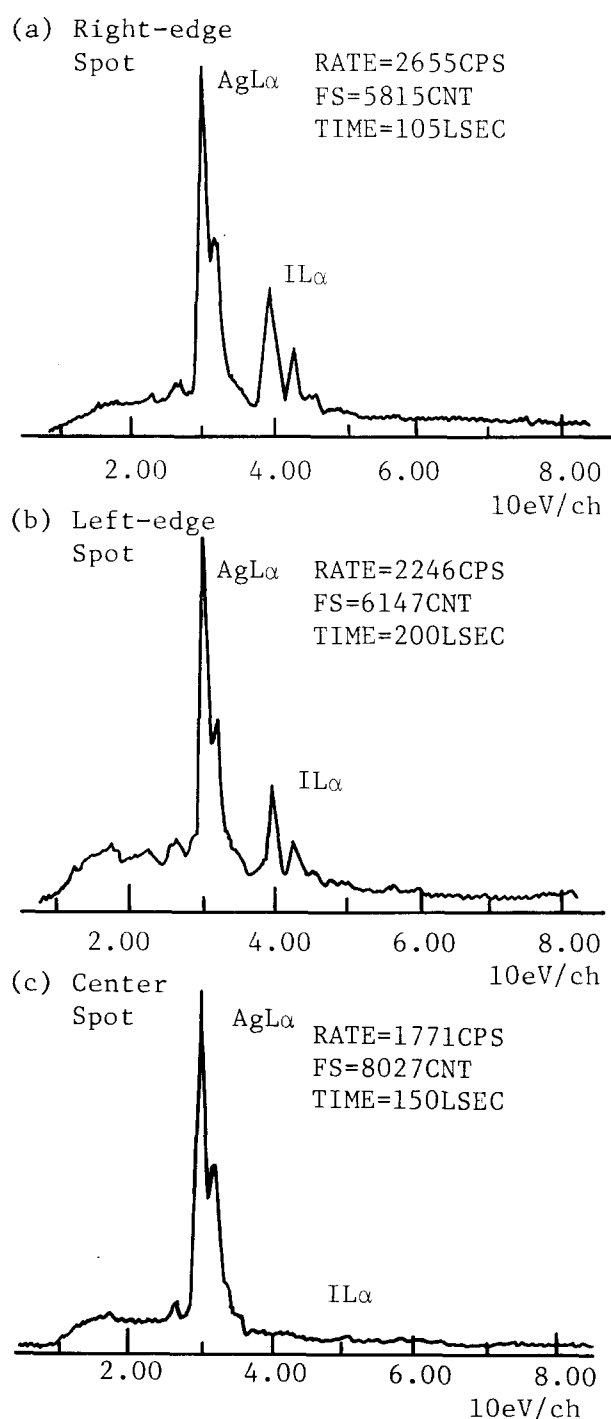


Figure 9 Spot analyses of Ag and I atoms for SV2-E2 fragment: (a) right-edge; (b) left-edge; (c) centre

0.82 mol/mol (see Table 2). Therefore, colloidal silver still remains in quaternized P2VP layers even after fixing treatment. Figure 11 shows the spot analyses of Ag, I and S atoms in SV2-E3 fragments ((a) right-edge; (b) left-edge; (c) centre). It was found from these spectra that the S contents at the right-edge and left-edge are larger than that at the centre. Consequently, $\text{Na}_2\text{S}_2\text{O}_3$ used at the fixing stage still exists near the surfaces after washing the film with water.

We carried out electrical conductivity measurements for diblock copolymer films possessing colloidal silver (Table 3). The conductivity of pure PS is ca. $10^{-17} \text{ S cm}^{-1}$ (see ref. 13). The σ_{\parallel} of SV-E films possessing colloidal silver is in the range of 10^{-5} – $10^{-4} \text{ S cm}^{-1}$. All films have a relatively high anisotropic conductivity with ca. six orders of magnitude. In previous work¹¹, we fabricated semiconducting materials composed of poly(*S-b*-quaternized 2VP) diblock copolymer films with lamellar microdomains. These films had an anisotropic conductivity with ca. eight orders of magnitude ($\sigma_{\parallel} = 10^{-6} \text{ S cm}^{-1}$ and $\sigma_{\perp} = 10^{-14} \text{ S cm}^{-1}$). The quaternized P2VP domains (counter ion, I^-) exhibit the nature of ionic conduction. The SV-E films prepared in this work show 10–100 fold values compared with poly(*S-b*-quaternized 2VP) films. The P2VP layers in SV-E films are constructed with a pyridinium ion–colloidal silver mixture. However, a large amount of I^- ions is excluded from the film in SV-E series. The entire ion carriers of the pyridinium units may be occupied by S_2O_3^- ions. So, it seems that the values of σ_{\parallel} listed in Table 3 reflect electron conduction among colloidal silver. However, the observed σ_{\parallel} value of SV-E series is extremely small compared with that of silver metal. Figure 12 shows a cross-sectional TEM micrograph of the SV2-E3 film. The black particles correspond to colloidal silver. It was found from this micrograph that silver particles distribute at intervals of a few nm from each other in the quaternized P2VP layer. Such an arrangement of silver particles leads to a decrease of the mean free path of electrons. In order to obtain materials possessing a high conductivity, it is necessary to introduce a large amount of colloidal silver into P2VP layers or to make continuous layers of colloidal silver. It seems difficult to achieve these purposes by using the methods employed in this work. We are investigating the preparation of highly electrical anisotropic block

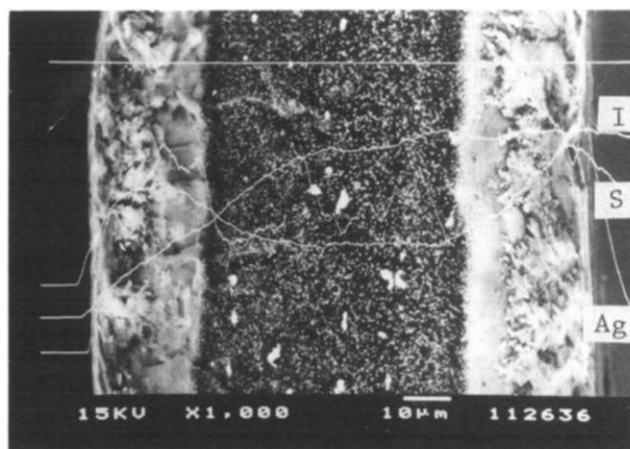


Figure 10 E.d.x. data (b.s.e. image of Ag atoms and concentration distributions of Ag, I and S atoms) of SV2-E3 fragment

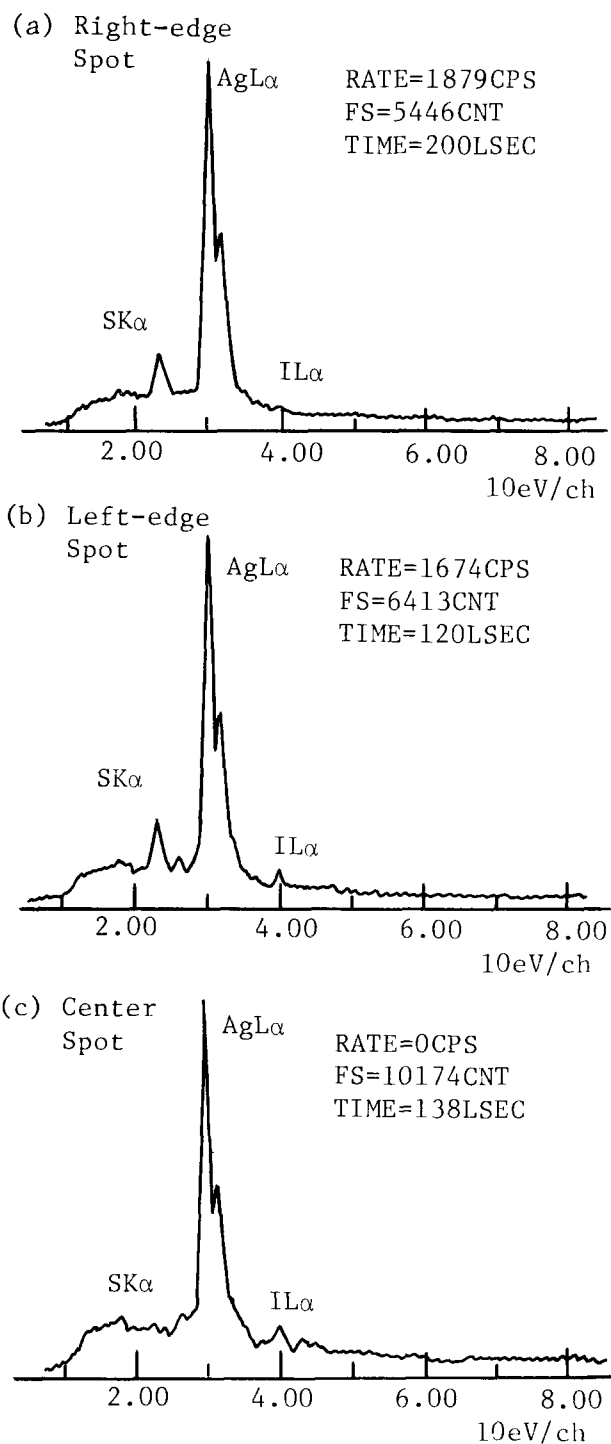


Figure 11 Spot analyses of Ag, I and S atoms for SV2-E3 fragment: (a) right-edge; (b) left-edge; (c) centre

copolymer films by varying the kinds of dopants. The results will be reported shortly.

ACKNOWLEDGEMENTS

We acknowledge, respectively, Mr R. Ooki and Mr T. Chiba, Faculty of Engineering, Tokyo Institute of

Table 3 Conductivities of diblock copolymer films possessing colloidal silver

Film code	Thickness of films (μm)	Conductivity (S cm^{-1}) ^a		Anisotropy $10^{-6} (\sigma_{\parallel}/\sigma_{\perp})$
		$10^5 \sigma_{\parallel}$	$10^{11} \sigma_{\perp}$	
SV1-E1	168	7.7	1.47	5.23
SV2-E1	124	2.7	1.38	1.94
SV2-E3	90	29.7	25.0	1.19

^a σ_{\parallel} , conductivity parallel to the film plane; σ_{\perp} , conductivity perpendicular to film plane

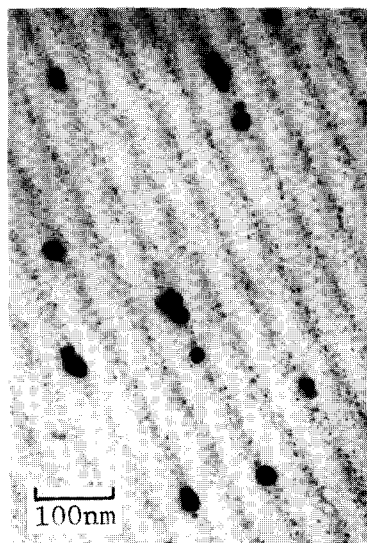


Figure 12 Cross-sectional TEM micrograph of the SV2-E3 film

Technology, for taking the e.d.x. data and the electron microscopic cross-sections of block copolymer films.

REFERENCES

- 1 Chance, R. R., Schacklette, L. W., Miller, G. G., Ivory, D. M., Sowa, J. M., Elsenbaumer, R. L. and Baughman, R. H. *Chem. Commun.* 1980, 348
- 2 Chien, J. C. W. 'Polyacetylene Chemistry, Physics and Material Science', Academic Press, New York, 1984
- 3 Wneck, G. E., Chien, J. C. W., Karasz, F. E. and Lilya, C. P. *Polymer* 1979, **20**, 1441
- 4 Gibson, H. W., Bailey, F. C., Epstein, A. J., Rommelmann, H. and Pochaw, J. M. *Chem. Commun.* 1980, 426
- 5 Lee, K. I. and Jopson, H. *Polym. Bull.* 1983, **10**, 105
- 6 Ikeno, S., Yokoyama, M. and Mikawa, H. *Polym. J.* 1978, **10**, 123
- 7 Möller, M. and Lenz, R. W. *Makromol. Chem.* 1989, **190**, 1153
- 8 Stanković, R. I., Lenz, R. W. and Karasz, F. E. *Eur. Polym. J.* 1990, **26**, 359
- 9 Shimidzu, T., Iyoda, T., Ando, M., Ohtani, A., Kaneko, T. and Honda, K. *Thin Solid Films* 1988, **106**, 67
- 10 Ishizu, K., Yamada, Y. and Fukutomi, T. *Polymer* 1990, **31**, 2047
- 11 Ishizu, K., Yamada, Y., Saito, R., Kanbara, T. and Yamamoto, T. *Polymer* 1992, **33**, 1816
- 12 Ishizu, K., Inagaki, K., Bessho, K. and Fukutomi, T. *Makromol. Chem.* 1984, **185**, 1169
- 13 Brandrup, J. and Immergut, E. H. (Eds) 'Polymer Handbook', Plenum Press, New York, 1975